



HAL
open science

On the Use of Vector Fitting and State-Space Modeling to Maximize the DC Power Collected by a Wireless Power Transfer System

Regis Rousseau, Florin Hutu, Guillaume Villemaud

► **To cite this version:**

Regis Rousseau, Florin Hutu, Guillaume Villemaud. On the Use of Vector Fitting and State-Space Modeling to Maximize the DC Power Collected by a Wireless Power Transfer System. AT-RASC 2018 - 2nd URSI Atlantic Radio conference, May 2018, Grande Canarie, Spain. pp.1-4. hal-01903660

HAL Id: hal-01903660

<https://hal.science/hal-01903660>

Submitted on 8 Nov 2018

HAL is a multi-disciplinary open access archive for the deposit and dissemination of scientific research documents, whether they are published or not. The documents may come from teaching and research institutions in France or abroad, or from public or private research centers.

L'archive ouverte pluridisciplinaire **HAL**, est destinée au dépôt et à la diffusion de documents scientifiques de niveau recherche, publiés ou non, émanant des établissements d'enseignement et de recherche français ou étrangers, des laboratoires publics ou privés.

On the Use of Vector Fitting and State-Space Modeling to Maximize the DC Power Collected by a Wireless Power Transfer System

Regis Rousseau, Florin Hutu, and Guillaume Villemaud

Univ Lyon, INSA Lyon, Inria, CITI, F-69621 Villeurbanne, France

Abstract

In this paper, the authors are proposing a way to maximize the DC power collected in the case of a wireless power transfer (WPT) scenario. Three main aspects are taken into account: the RF (radio frequency) source, the propagation channel and the rectifier as the main part of the energy collecting circuit. This problem is formulated as a convex optimization one. Then, as a first step towards solving this problem, a rectifier circuit was simulated by using Keysight's ADS software and, by using a classical model identification strategy i. e. Vector Fitting (VF) algorithm, the state-space model of the passive parts of this rectifier were extracted. In order to verify the extracted model, S_{11} input reflection coefficients and DC output voltages of the original circuit and the state-space model are compared.

1 Introduction

With the advent of the Internet of Things (IoT), the problem of power supplying the connected objects became crucial. Indeed, a plethora of IoT applications are demanding the deployment of such objects in environments in which classical power supplying strategies (battery, electricity grid, etc.) are impossible to implement. Minimizing the energy consumption of these connected objects, energy harvesting strategies (EH) or even wireless power transfer (WPT) are the main solutions studied nowadays in order to overcome this issue.

The massive adoption of smartphones has encouraged the proliferation of IoT to become part of our daily lives. These billions of connected objects pose a major environmental problem: their batteries because they have limited lifetime and, moreover, in the majority of applications, it is impossible to replace them. The general objective is to conceive autonomous, batteryless connected objects or at least, to significantly extend their lifetime.

As stated, WPT is one of the solutions to overcome the connected objects' power supply limitations. It is employing an intentional electromagnetic (EM) signal, transmitted with a certain amount of power in order to remotely power supply the connected devices [1]. In most of the cases, the emitted power level is known and most of the time is constant, which makes it possible to carry out the optimal design of the RF to DC rectifier circuit.

Several works proposed to improve the RF-DC conversion efficiency of the rectifier circuits by selecting the most suitable waveform for the transmitted EM signal. In [2, 3], the use of multi-tones or chaotic signals has been explored as a way to improve the conversion efficiency in WPT systems. This work has shown that signals with a time varying envelope can provide better efficiency because they are able to activate the RF-DC receivers for lower average input power levels compared to constant envelope signals.

In [4], the author shown how the use of waveforms specifically selected or conceived in WPT systems can lead to better RF-DC conversion efficiency. Signals with different waveforms such as the Orthogonal Frequency-Division Multiplexing (OFDM) signals, white noise and chaotic ones have been sent in order to test the performance of an RF-DC rectifier circuit. Performance is also compared with constant and single carrier envelope signals. Once again, high Peak to Average Power Ratio (PAPR) signals demonstrated their efficiency compared to Continuous Wave (CW) one.

Moreover, in [5] the authors described the behavior of rectifier RF-DC subjected to high RF input power. The efficiency degrades in the high input power region, typically for a power above -10 dBm. On the other hand, rectifier efficiency is significantly enhanced in the lower input power region, basically start-up region of a Schottky diode. In the middle input power region, the square law region at low level signal, signal modulation slightly improves the efficiency.

In the same way, the authors in [6] propose a method to improve the efficiency of WPT by using the effect of opportunistic scheduling. In this analysis and this case study, it becomes necessary to have a global view of the WPT system, both the channel and the circuit to maximize the collected energy.

Consequently, an accurate model extraction of a rectifier circuit is necessary to study the impact of modulated signal on the DC output power maximization, and this for a very large scale of RF input power level (typically on the square law and linear detection of the diode). A solution is to characterize the RF to DC rectifier by the use of X-parameters [7] and to have a model taking into account the harmonics due to the nonlinearity of the rectifier.

This paper is structured as follows: the section II presents the motivation of having a global view of WPT systems. A state-space model for wireless power system (WPS) is presented in section III and section IV presents simulation results and a comparison between the original RF to DC rectifier circuit and the extracted RF to DC rectifier circuit. Conclusions and future directions of this work are given in section V.

2 Global view of a wireless power transfer system

Figure 1 presents the proposed global framework of the WPT system. In order to maximize the collected energy, a similar state-space model will characterize the rectifying circuit and the propagation channel. Knowing the characteristics and the mathematical model corresponding to the propagation channel and the RF to DC rectifier, the generated RF waveform will be adapted for a maximum efficiency.

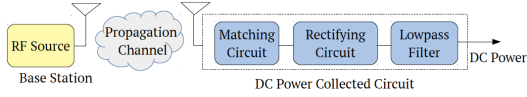


Figure 1. Example of a WPT system. Base station transmits an optimized signal taking into account the propagation channel and the rectifier's behavior to maximize the DC output power.

We suppose that the RF generator's output signal is a multi-carrier one :

$$x(t) = \Re \left(\sum_{n=0}^{N-1} S_n \cdot e^{j(\omega_n t + \phi_n)} \right) \quad (1)$$

where S_n and ϕ_n refer to the amplitude and phase of the n^{th} sub-carrier at the pulsation ω_n , respectively.

S_n and ϕ_n can be set up to give the maximum of output DC power knowing the maximum output power which can be emitted by the base station. To do so, each element of the WPT system is modeled by using a state-space model representation. Some papers are demonstrating that a propagation channel can be modeled by a state-space model [8]. If we can use the same representation for the rectifier, the WPT can be seen as a close loop control system, as shown in figure 2.

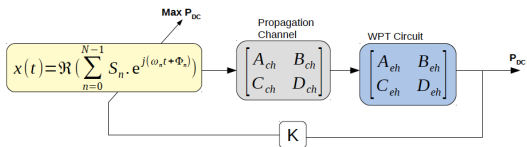


Figure 2. A WPT system seen as a closed loop. Propagation channel and rectifying circuit are modeled by their respective state-space models.

3 Model of a Conventional Rectifier Circuit

The first step in solving this problem is to identify the models of the communication channel and of the rectifier circuit. In the following, the rectifier which is used in our study has a conventional structure, as shown in Figure 3.

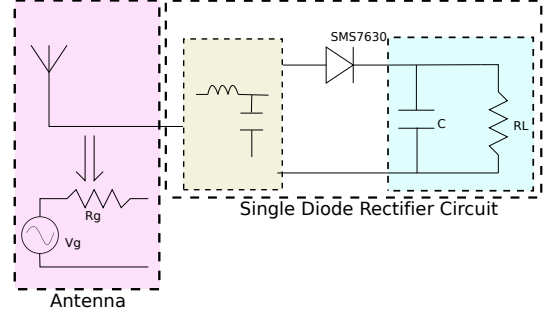


Figure 3. Simple single diode rectifier circuit topology : receiver antenna which is modeled by a 1-Tone generator in series with a 50Ω resistor, matching network, a SMS7630 Schottky diode in series, and an R-C cell.

The studied WPT system consists of four elements : a RF source, an impedance matching network, a rectifier and a R-C cell. RF source is a 1-tone generator and generates a continuous wave at 2.45 GHz.

The lumped components of the L -matching networks are optimized to guarantee an input reflection coefficient between -20 dB to -26 dB for an input signal of 2.45 GHz having a 40 MHz bandwidth and a -40 dBm input power level. The rectifying circuit is composed of a SMS7630 Schottky diode. Because of its nonlinear property, the Schottky diode transforms the input signal into a mono alternating signal which is smoothed by the capacitor C. The resistor R_L represents the load.

In order to represent the WPT circuit as a state-space model, the vector fitting algorithm, presented in [9], is used to create a state-space model of all linear networks of the rectifier : impedance matching network, linear parasitic components of SMS7630 Schottky diode, and R-C cell. VF approximates each linear quadripole of the system by a rational function with its own poles and residues. The output of S-parameters data in the frequency domain is also associated with a corresponding state-space model. S-parameters of one quadripole can then be modeled as a sum of the residues, r_k , over first-order poles, p_n [10, 11]:

$$H(s) = \sum_{k=1}^N \frac{r_k}{s - p_k} + d \quad (2)$$

$$H(s) = \mathbf{C}(s \cdot \mathbb{I} - \mathbf{A})^{-1} \mathbf{B} + \mathbf{D} \quad (3)$$

where N denotes the VF order and $s = j\omega$. Considering a n-port system and VF of order N, the total number of

state variables m will be $m = n \times N$. Thus, the corresponding state-space model will have the following properties: \mathbf{A} is an $m \times m$ diagonal matrix containing the N poles p_n repeated n times, \mathbf{B} is an $m \times n$ matrix and contains only ones or zeros, \mathbf{C} is composed of the r_{pqn} residues and is an $n \times m$ matrix, and \mathbf{D} is a $n \times n$ matrix and is composed of real constants.

4 Model Validation

VF described in the previous section is performed to extract the state-space model of the rectifier's linear parts, except the SMS7630 diode which is a nonlinear one.

The matching circuit is composed of two L -matching networks. Inductors and capacitors of the two L -networks have been optimized and the input reflection coefficient gives a minimum of -25 dB at 2.455 GHz and a maximum value of -20 dB at 2.422 GHz.

Figure 4 shows the input reflection coefficient as function of frequency, from 2.4 GHz to 2.5 GHz for $N = 2, 3, 4$ and 5. As can be seen, the model giving the best similarity with the initial S_{11} parameter is for $N = 5$. For $N = 3$ and $N = 4$, the models are similar but the error is increasing. As for $N = 2$, even the shape of the curve differs, which shows the importance of the initial choice of the VF order to the execution of the VF algorithm.

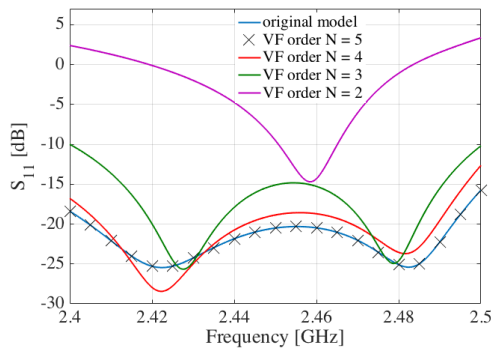


Figure 4. Comparison of original rectifier's reflection coefficient and the reflection coefficient of the rectifier's models.

Figure 5 presents the DC output voltage as function of RF input power, from -50 dBm to 0 dBm. In this case, the choice of the value of N seems less impacting on the expected result. There is a superposition of the curves for $N = 3, 4$, and 5 over the entire input power range. The expected result being a perfect match of the curves resulting from the model with the original circuit, for an input power lower than -20 dBm, which corresponds to the square law region of the diode. A value 3, 4 or 5 of N can be chosen because the values coincide. When the diode works beyond this RF input power, values are diverging as input power increases. $N = 2$ also seems not to be a correct estimate for

replacing the VF model with the original. Table 1 presents the RMS errors from the VF for the different chosen sizes.

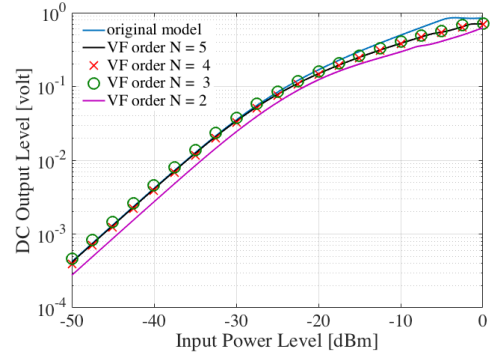


Figure 5. Evolution of DC output voltage as a function of input power level for $R_L = 10k\Omega$ and $C = 220nF$.

Table 1. Resulting RMS-error of the VF

N	Error returned by VF algorithm			
	IMN	AP	CP	R-C cell
1	0.4495	2.05e-4	0.0026	0.0159
2	0.2054	1.55e-6	1.84e-5	0.0149
3	0.0224	2.88e-10	2.88e-10	0.004
4	0.0226	2.88e-10	2.88e-10	0.004
5	2.88e-10	2.88e-10	2.88e-10	0.004

IMN: impedance matching network. AP: anode parasitics. CP: cathode parasitics. R-C cell: resistor-capacitor cell.

To illustrate the results given by the VF algorithm, the impedance matching network's state-space model is given below for $N = 3$ and $n = 2$. The order of the state-space model will therefore be the size of the matrix \mathbf{A} , thus of order $m = 6$.

$\mathbf{A} = 1.0e+10^*$

$$\begin{bmatrix} -1.48 & 0 & 0 & 0 & 0 & 0 \\ 0 & -0.03 + 1.55i & 0 & 0 & 0 & 0 \\ 0 & 0 & -0.03 - 1.55i & 0 & 0 & 0 \\ 0 & 0 & 0 & -1.48 & 0 & 0 \\ 0 & 0 & 0 & 0 & -0.03 + 1.55i & 0 \\ 0 & 0 & 0 & 0 & 0 & -0.03 - 1.55i \end{bmatrix}$$

$\mathbf{C} = 1.0e+10^*$

$$\begin{bmatrix} 2.036 & 0.004 \pm 0.015i & -0.054 & 0.007 \pm 0.003i \\ -0.054 & 0.007 \pm 0.003i & 0.284 & -0.017 \pm 0.021i \end{bmatrix}$$

$$\mathbf{B}^T = \begin{bmatrix} 1 & 1 & 1 & 0 & 0 & 0 \\ 0 & 0 & 0 & 1 & 1 & 1 \end{bmatrix} \quad \mathbf{D} = \begin{bmatrix} -0.9989 & 0.0402 \\ 0.0402 & 0.4501 \end{bmatrix}$$

5 Conclusion

In this paper, a framework for modeling WPT was proposed. This study is shown the viability of using VF method to model of the rectifier's linear part. This linear part was modeled in the frequency domain as a rational model on pole-residue form and a corresponding state-space model

was extracted. Future works will focus on nonlinear state-space model of rectifying device and the extraction of the suitable multi carrier signal able to maximize the collected power.

6 Acknowledgements

The authors acknowledge the support of the INSA LYON-SPIE ICS research chair.

References

- [1] N. Shinohara, "Power without Wires," *IEEE Microwave Magazine*, **12**, dec 2011, pp. 64–73, doi: 10.1109/MMM.2011.942732.
- [2] A. Collado and A. Georgiadis, "Optimal Waveforms for Efficient Wireless Power Transmission," *IEEE Microwave and Wireless Components Letters*, **24**, May 2014, pp. 354–356, doi: 10.1109/LMWC.2014.2309074.
- [3] A. Boaventura and N. Carvalho, "Spatially-combined Multisine Transmitter for Wireless Power Transmission," *IEEE Wireless Power Transfer*, July 2013, pp. 21–24, doi: 10.1109/WPT.2013.6556872.
- [4] B. Clerckx and E. Bayguzina, "Waveform Design for Wireless Power Transfer," *IEEE Transactions on Signal Processing*, **64**, August 2016, pp. 6313–6328, doi: 10.1109/TSP.2016.2601284.
- [5] K. Nishikawa and H. Sakaki, "Impact of Modulation Scheme on Rectifier RF-DC Efficiency and Optimal Signal Control Technique," *IEEE International Microwave and RF Conference*, February 2016, pp. 288–291, doi: 10.1109/IMaRC.2015.7411443.
- [6] M. Xia and S. Aissa, "Effect of Opportunistic Scheduling on the Efficiency of Wireless Power Transfer," *IEEE Global Communications Conference*, February 2014, pp. 4288–4293, doi: 10.1109/GLOCOM.2014.7037481.
- [7] A. Boaventura and N. Carvalho, "Using X-parameters to Model RFID Energy Harvesting Circuits," *Conference on Antennas and Propagation*, May 2011, pp. 2819–2822.
- [8] C. Zhang and R. Bitmead, "State Space Modeling for MIMO Wireless Channels," *IEEE International Conference on Communications*, August 2005, pp. 2297–2301, doi: 10.1109/ICC.2005.1494745.
- [9] Skyworks, "Circuit Models for Plastic Packaged Microwave Diodes," *APN1001 Application Note*, July 2005 [200311 Rev.A]
- [10] B. Gustavsen, "Computer Code for Rational Approximation of Frequency Dependent Admittance Matrices," *IEEE Transaction on Power Delivery*, **17**, October 2002, pp. 1093–1098, doi: 10.1109/TPWRD.2002.803829.
- [11] B. Gustavsen, "Improving the Pole Relocating Properties of Vector Fitting," *IEEE Transaction on Power Delivery*, **31**, June 2006, pp. 1587–1592, doi: 10.1109/TPWRD.2005.860281.